

# Pomeron pole plus grey disk model : real parts, inelastic cross sections and LHC data

S. M. Roy<sup>1, \*</sup>

<sup>1</sup>*HBCSE, Tata Institute of Fundamental Research, Mumbai*

I propose a two component analytic formula  $F(s, t) = F^{(1)}(s, t) + F^{(2)}(s, t)$  for  $(ab \rightarrow ab) + (ab \rightarrow \bar{a}\bar{b})$  scattering at energies  $\geq 100\text{GeV}$ , where  $s, t$  denote squares of c.m. energy and momentum transfer. It saturates the Froissart-Martin bound and obeys Auberson-Kinoshita-Martin (AKM) [1] [2] scaling. I choose  $ImF^{(1)}(s, 0) + ImF^{(2)}(s, 0)$  as given by Particle Data Group (PDG) fits [3],[4] to total cross sections, corresponding to simple and triple poles in angular momentum plane. The PDG formula is extended to non-zero momentum transfers using partial waves of  $ImF^{(1)}$  and  $ImF^{(2)}$  motivated by Pomeron pole and 'grey disk' amplitudes and constrained by inelastic unitarity.  $ReF(s, t)$  is deduced from real analyticity: I prove that  $ReF(s, t)/ImF(s, 0) \rightarrow (\pi/\ln s)d/d\tau(\tau ImF(s, t)/ImF(s, 0))$  for  $s \rightarrow \infty$  with  $\tau = t(\ln s)^2$  fixed, and apply it to  $F^{(2)}$ . Using also the forward slope fit by Schegelsky-Ryskin [5], the model gives real parts, differential cross sections for  $(-t) < .3\text{GeV}^2$ , and inelastic cross sections in good agreement with data at  $546\text{GeV}, 1.8\text{TeV}, 7\text{TeV}$  and  $8\text{TeV}$ . It predicts for inelastic cross sections for  $pp$  or  $\bar{p}p$ ,  $\sigma_{inel} = 72.7 \pm 1.0\text{mb}$  at  $7\text{TeV}$  and  $74.2 \pm 1.0\text{mb}$  at  $8\text{TeV}$  in agreement with  $pp$  Totem [7][8] [9][10] experimental values  $73.1 \pm 1.3\text{mb}$  and  $74.7 \pm 1.7\text{mb}$  respectively, and with Atlas [12][13][14][15] values  $71.3 \pm 0.9\text{mb}$  and  $71.7 \pm 0.7\text{mb}$  respectively. The predictions  $\sigma_{inel} = 48.1 \pm 0.7\text{mb}$  at  $546\text{GeV}$  and  $58.5 \pm 0.8\text{mb}$  at  $1800\text{GeV}$  also agree with  $\bar{p}p$  experimental results of Abe et al [47]  $48.4 \pm .98\text{mb}$  at  $546\text{GeV}$  and  $60.3 \pm 2.4\text{mb}$  at  $1800\text{GeV}$ . The model yields for  $\sqrt{s} > 0.5\text{TeV}$ , with PDG2013 [4] total cross sections, and Schegelsky-Ryskin slopes [5] as input,  $\sigma_{inel}(s) = 22.6 + .034\ln s + .158(\ln s)^2\text{mb}$ , and  $\sigma_{inel}/\sigma_{tot} \rightarrow 0.56$ ,  $s \rightarrow \infty$ , where  $s$  is in  $\text{GeV}^2$  units. Continuation to positive  $t$  indicates an 'effective'  $t$ -channel singularity at  $\sim (1.5\text{GeV})^2$ , and suggests that usual Froissart-Martin bounds are quantitatively weak as they only assume absence of singularities upto  $4m_\pi^2$ .

PACS numbers: 13.85.Dz, 13.85.Lg, 13.85.Hd, 11.55.Jy, 12.40.Nn

**Introduction.** Precision measurements of  $pp$  cross sections at LHC [7] [8][9][10][11][12][13][14][15][16], and in cosmic rays [17] motivate me to present a model for  $ab \rightarrow ab$  scattering amplitude at c.m. energies  $\sqrt{s} > 100\text{GeV}$  described by an analytic formula containing very few parameters. Neglecting terms with a power decrease at high  $s$ , the Particle Data Group (PDG) fits to total cross sections [3],[4] are the sum of one constant component and another rising as  $(\ln s)^2$ , corresponding to a simple pole and a triple pole at  $J = 1$  in the angular momentum plane,

$$\begin{aligned}\sigma_{tot}^{ab} &= \sigma_{tot}^{(1),ab} + \sigma_{tot}^{(2),ab}, \\ \sigma_{tot}^{(1),ab} &= P^{ab}, \sigma_{tot}^{(2),ab} = H(\ln s/s_M^{ab})^2.\end{aligned}\quad (1)$$

I propose that, analogously, the full amplitude  $F(s, t) = F^{(1)}(s, t) + F^{(2)}(s, t)$ , where,  $F^{(1)}$  is a Pomeron simple pole amplitude,  $ImF^{(2)}$  has partial waves with a smooth cut-off at impact parameter  $b = R(s)$  corresponding to a grey disk and  $ReF^{(2)}(s, t)$  is calculated from a theorem I prove using real analyticity and Auberson-Kinoshita-Martin (AKM) [1] [2] scaling for  $s \rightarrow \infty$  with fixed  $t(\ln s)^2$ . Inelastic unitarity is tested using inputs of total cross sections, forward slopes and Pomeron parameters.

Only inputs leading to unitary amplitudes are accepted. Model predictions for inelastic cross sections, near forward real parts and differential cross sections agree with existing data and can be tested against future LHC experiments.

**Froissart-Martin bound basics.** Froissart [18], from the Mandelstam representation, and Martin [19], from axiomatic field theory, proved that the total cross-section  $\sigma_{tot}(s)$  for two particles  $a, b$  to go to anything must obey the bound,

$$\sigma_{tot}(s) \leq_{s \rightarrow \infty} C [\ln(s/s_0)]^2, \quad (2)$$

where  $C, s_0$  are unknown constants. It was proved later [20] that  $C = 4\pi/(t_0)$ , where  $t_0$  is the lowest singularity in the  $t$ -channel. This bound has been extremely useful in theoretical investigations [21] [22] and high energy models [23] [24][25][26][27][28][29][30][31][32]. Analogous bounds on the inelastic cross section have been obtained by Martin [33] and Wu et al [34]; for pion-pion case, Martin and Roy obtained bounds on energy averaged total [35] and inelastic cross sections [36] which also fix the scale factor  $s_0$  in these bounds.

**Normalization.** For the  $ab \rightarrow ab$  scattering amplitude  $F(s, t)$ ,  $a \neq b$ , with  $k = \text{c.m. momentum}$ , and  $z =$

\*Electronic address: smroy@hbcse.tifr.res.in

$$1 + t/(2k^2),$$

$$F(s, t) = \sqrt{s}/(4k) \sum_{l=0}^{\infty} (2l+1) P_l(z) a_l(s),$$

$$\sigma_{tot}(s) = 4\pi/(k^2) \sum_{l=0}^{\infty} (2l+1) \text{Im} a_l(s)$$

$$\frac{d\sigma}{dt} = \frac{\pi}{k^2} \frac{d\sigma}{d\Omega}(s, t) = \frac{\pi}{k^2} \left| 4 \frac{F(s, t)}{\sqrt{s}} \right|^2. \quad (3)$$

with the inelastic unitarity constraint  $\text{Im} a_l(s) \geq |a_l(s)|^2$ . For identical particles  $a = b$ , the partial waves  $a_l(s) \rightarrow 2a_l(s)$  in the above partial wave expansions for  $F(s, t)$ , and  $\sigma_{tot}(s)$ , but the odd partial waves are zero. We have the same formulae for the unitarity constraint, and the differential cross section as given above.

At high energy, using  $a_l(s) \equiv a(b, s)$ ,  $l = bk$ , where  $b$  is the impact parameter, and  $P_l(\cos\theta) \sim J_0((2l+1)\sin(\theta/2)) + O(\sin^2(\theta/2))$ , we have the impact parameter representaion,

$$F(s, t) = k\sqrt{s}/2 \int_0^{\infty} b db a(b, s) J_0(b\sqrt{-t})$$

$$\sigma_{tot} = 8\pi \int_0^{\infty} b db \text{Im} a(b, s); \quad \sigma_{el} = 8\pi \int_0^{\infty} b db |a(b, s)|^2$$

$$d\sigma/dt = 4\pi \left| \int_0^{\infty} b db a(b, s) J_0(b\sqrt{-t}) \right|^2, \quad (4)$$

There exist very good fits to high energy data [37] [38] with a very large number of free parameters. There are also very good eikonal based models involving several free parameters [23] [24][25][26][27][28][29][30][31][32]. The recent eikonal based model of Block and Halzen (BH)[39][40] uses high energy data to guess the glue-ball mass and to probe whether the proton is a black disk.

**A two component partial wave model.** I present a two component model with very few parameters and with analytic formulae for the total amplitude incorporating unitarity-analyticity constraints, PDG total cross sections and the AKM scaling theorem.

**Imaginary parts.** I use the two component PDG total cross section fit. I propose that in the impact parameter picture, the Imaginary part  $\text{Im} a(b, s)$  of the partial waves at fixed  $s$  is also a sum of two components, one part  $\text{Im} a^{(1)}(b, s)$  a Gaussian corresponding to a Pomeron pole, and the other  $\text{Im} a^{(2)}(b, s)$  a polynomial of degree  $2n$  in  $b^2$  with a smooth cut-off at  $b = R(s)$ ,  $n$  being a positive integer. so that  $\text{Im} a^{(2)}(b, s)$  is continuous and has continuous derivative at  $b = R(s)$ . The second component corresponds to a “grey” disk with cross section rising as  $(\ln s)^2$ ,

$$\text{Im} a(b, s) = \text{Im} a^{(1)}(b, s) + \text{Im} a^{(2)}(b, s),$$

$$\text{Im} a^{(1)}(b, s) = C(s) \exp(-2b^2/D^2(s)),$$

$$\text{Im} a^{(2)}(b, s) = E(s)(1 - b^2/R^2(s))^{2n} \theta(R(s) - b), \quad (5)$$

where  $\theta(x) = 1$ , for  $x \geq 0$ , and 0 otherwise. The unitarity constraints are,

$$C(s) \geq 0, E(s) \geq 0, 0 \leq C(s) + E(s) \leq 1. \quad (6)$$

In Eq.(5) we take the simplest choice  $n = 1$  in this paper. Using the ansatz for  $\text{Im} a^{(1)}(b, s)$ , integrating over  $b$ , and matching the result for  $\text{Im} F^{(1)}(s, t)$  with the standard small  $t$  Pomeron amplitude,

$$F^{(1)}(s, t) = \frac{k\sqrt{s}}{16\pi} \sigma_{tot}^{(1)} \exp(tb_P + t\alpha' \ln s)(i + t\frac{\pi}{2}\alpha'), \quad (7)$$

we obtain,

$$D^2(s) = 8(b_P + \alpha' \ln s), \quad C(s) = \sigma_{tot}^{(1)}/(2\pi D^2(s)). \quad (8)$$

Since  $\sigma_{tot}^{(1)}$  is a constant,  $C(s) \rightarrow \text{const}/(\ln s)$ ,  $s \rightarrow \infty$  for  $\alpha' \neq 0$ . Similarly, the ansatz for  $\text{Im} a^{(2)}(b, s)$  with  $n = 1$  yields,

$$\text{Im} F^{(2)}(s, t) = E(s) \frac{4k\sqrt{s}}{q^3 R(s)} J_3(qR(s)), \quad q \equiv \sqrt{-t}, \quad (9)$$

where  $J_m(x)$  denotes the Bessel function of order  $m$ . Hence,

$$\sigma_{tot}^{(2)}(s) = \frac{16\pi}{k\sqrt{s}} \text{Im} F^{(2)}(s, 0) = \frac{4\pi}{3} E(s) R^2(s). \quad (10)$$

Thus,  $C(s)D^2(s)$  and  $E(s)R^2(s)$  are determined from the PDF total cross section fits using Eqns.(8) and (10) respectively. A nice feature of the model is that the above unitarity constraints (6) as well as a stronger version including real parts can be readily tested, and provide acceptability criteria for extrapolations of experimental data for  $pp$  scattering.

**Theorem on Real parts.** Let  $F(s, t) = F(y; t)$ ,  $y \equiv ((s - u)/2)^2$  be an  $s - u$  symmetric amplitude, with asymptotic behaviour  $|s|(\ln |s|)^\gamma |\phi(\tau)|$ ,  $\tau \equiv t(\ln |s/s_0|)^\beta$ , where  $\phi(\cdot)$  is a real analytic function of it's argument and  $\phi(0) = 1$ . For fixed physical  $t$ ,  $F$  is real analytic in the cut- $y$  plane with only a right-hand cut from  $(2m_a m_b + t/2)^2$  to  $\infty$ .  $F$  must be real for  $y = |y| \exp(i\pi)$ , i.e.  $s \rightarrow |s| \exp(i\pi/2)$ , and hence replacing  $|s| \rightarrow s \exp(-i\pi/2)$ , we have for  $s \rightarrow \infty$ ,  $\tau$  fixed,

$$F(s, t) \sim -C' s \exp(-i\pi/2)(\ln(s/s_0) - i\pi/2)^\gamma \times \phi(t(\ln(s/s_0) - i\pi/2)^\beta) \quad (11)$$

Expanding in powers of  $1/\ln s$  at fixed  $\tau$  we get,

$$\frac{\text{Im} F(s, t)}{\text{Im} F(s, 0)} \rightarrow \phi(\tau); \quad (12)$$

$$\frac{\text{Re} F(s, t)}{\text{Im} F(s, 0)} \rightarrow \frac{\pi}{2 \ln(s/s_0)} (\gamma \phi(\tau) + \beta \tau \phi'(\tau)), \quad (13)$$

$$\frac{\text{Re} F(s, t)}{s} \rightarrow (\pi/2) \left( \frac{\partial(\text{Im} F(s, t)/s)}{\partial(\ln(s/s_0))} \right); \quad (14)$$

$$\text{Re} a(b, s) \rightarrow (\pi/2) \frac{\partial(\text{Im} a(b, s))}{\partial \ln(s/s_0)}, \quad (15)$$

where, due to linearity, the last two equations also hold for a superposition of terms of the form (11), e.g.  $F^{(1)} + F^{(2)}$ . Note that, (i)  $\text{Re} F(s, 0)/\text{Im} F(s, 0)$  agrees with the Khuri-Kinoshita theorem [41], (ii) the case  $\beta = \gamma = 1$

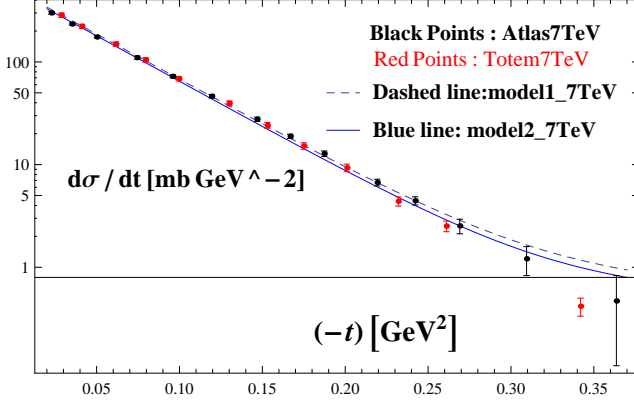


FIG. 1: Model predictions for pp elastic differential cross sections  $d\sigma/dt$  at 7TeV, with parameters  $b_P = 3.8GeV^{-2}$ ,  $\alpha' = 0.07GeV^{-2}$ , forward slope from Schegelsky - Ryskin fit [5], input  $\sigma_{tot}$  from PDG (2005)[3] (dashed curve), and input  $\sigma_{tot}$  from PDG (2013)[4] (solid curve), show excellent agreement with experimental values from the Totem [7][8][9][10] and Atlas [12][13][14][15] collaborations for  $|t| < 0.3GeV^2$ .

agrees with Martin's geometrical scaling formula [42] [43]. (iii) When  $\sigma_{tot} \sim (\ln s)^2$ ,  $\gamma = \beta = 2$ , the AKM theorem and Auberson-Roy theorem [1][2] guarantee the scaling of  $ImF(s, t)/ImF(s, 0)$  with  $\phi(\tau)$  being an entire function of order half. The crucial new result is the formula (13) for  $ReF(s, t)$ . In turn, this yields for the partial waves of  $F^{(2)}$ , if  $b^2 Im a^{(2)}(b, s) \rightarrow 0$  for  $b \rightarrow \infty$ ,

$$Re a^{(2)}(b, s) \rightarrow \frac{-\pi}{2 \ln(s/s_0)} b \frac{\partial}{\partial b} Im a^{(2)}(b, s), s \rightarrow \infty. \quad (16)$$

However, in view of the slow approach to asymptotics, the formula (15) for  $Re a(b, s)$  involving derivative over  $\ln s$  is preferable for computations, as it holds also for  $F^{(1)} + F^{(2)}$ .

**The total amplitude.** Consistent with (13) for  $\gamma = \beta = 2$ , i.e.  $\tau = t(\ln |s/s_0|)^2$ , I adopt the ansatz,

$$\frac{ReF^{(2)}(s, t)}{ImF^{(2)}(s, 0)} = \frac{\pi}{\ln(s/s_0)} \frac{d}{d\tau} \left( \tau \frac{ImF^{(2)}(s, t)}{ImF^{(2)}(s, 0)} \right). \quad (17)$$

For simplicity, I choose the scale factor  $s_0$  to be the same as in the PDG(2005)[3] fit for  $pp$  total cross section,  $\sqrt{s_0} = 5.38GeV$ . Substituting the expression for  $ImF^{(2)}(s, t)$  I obtain,

$$\begin{aligned} \frac{16\pi}{k\sqrt{s}} F^{(2)}(s, t) &= \sigma_{tot}^{(2)}(s) \left[ \frac{\pi}{\ln(s/s_0)} \right. \\ &\times \frac{8J_2(qR(s)) - 16J_4(qR(s))}{q^2 R^2(s)} + i \frac{48J_3(qR(s))}{(qR(s))^3} \left. \right]. \end{aligned} \quad (18)$$

The total amplitude  $F(s, t) = F^{(1)}(s, t) + F^{(2)}(s, t)$  is now completely specified (analytically) by adding  $F^{(1)}(s, t)$  given by (7). The important parameter  $R^2(s)$  is determined from the experimental slope parameter  $B(s) =$

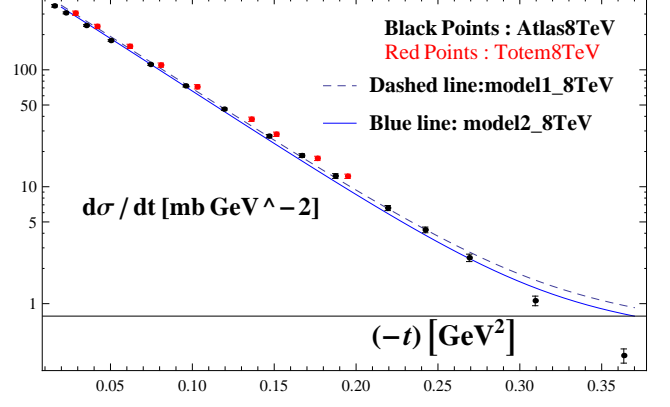


FIG. 2: Model predictions for pp elastic differential cross sections  $d\sigma/dt$  at 8TeV, with parameters  $b_P = 3.8GeV^{-2}$ ,  $\alpha' = 0.07GeV^{-2}$ , forward slope from Schegelsky - Ryskin fit [5], input  $\sigma_{tot}$  from PDG (2005)[3] (dashed curve), and input  $\sigma_{tot}$  from PDG (2013)[4] (solid curve), show excellent agreement with experimental values from the Totem [7][8][9][10] and Atlas [12][13][14][15] collaborations for  $|t| < 0.3GeV^2$ .

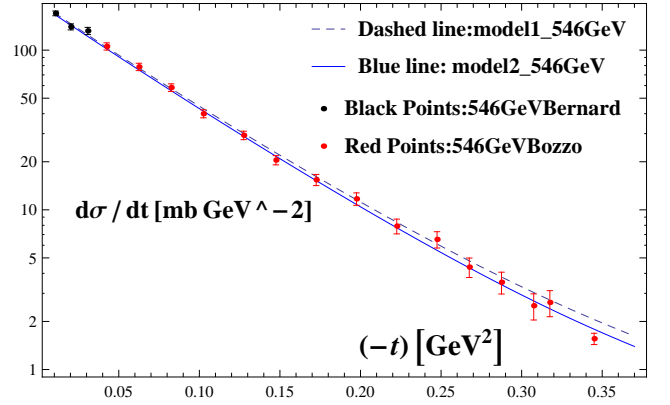


FIG. 3: Model predictions for  $\bar{p}p$  elastic differential cross sections  $d\sigma/dt$  at 546GeV, with parameters  $b_P = 3.8GeV^{-2}$ ,  $\alpha' = 0.07GeV^{-2}$ , forward slope from Schegelsky - Ryskin fit [5], input  $\sigma_{tot}$  from PDG (2005)[3] (dashed curve), and input  $\sigma_{tot}$  from PDG (2013)[4] (solid curve), show good agreement with experimental values from UA4 collaborations, D. Bernad et al[44] and M. Bozzo et al [45] for  $|t| < 0.3GeV^2$ .

$(d/dt)(\ln d\sigma/dt)|_{t=0}$ , if the Pomeron parameters  $b_P, \alpha'$  are known,

$$\begin{aligned} &R^2(s) \left( \epsilon(s) \sigma_{tot}^{(2)}(s)^2 + \frac{1}{2} \sigma_{tot}^{(2)}(s) \sigma_{tot}(s) \right) \\ &= 4B(s) \left( \epsilon(s) \sigma_{tot}^{(2)}(s)^2 + \sigma_{tot}(s)^2 \right) \\ &- \sigma_{tot}^{(1)} \sigma_{tot}(s) D^2(s) - 4\pi \alpha' \sqrt{\epsilon(s)} \sigma_{tot}^{(1)} \sigma_{tot}^{(2)}(s), \end{aligned} \quad (19)$$

where, we denote  $\sqrt{\epsilon(s)} \equiv \pi/\ln(s/s_0)$ . For the experimental slope parameter I shall use the fits  $B(M, s)$  to all  $pp$  data, with  $M = 1, 2$ ,  $B(1, s)$  by Okorokov [6] and

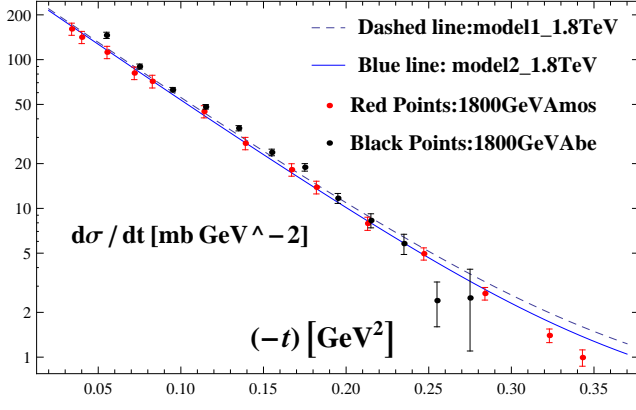


FIG. 4: Model predictions for  $\bar{p}p$  elastic differential cross sections  $d\sigma/dt$  at  $1800\text{GeV}$ , with parameters  $b_P = 3.8\text{GeV}^{-2}$ ,  $\alpha' = 0.07\text{GeV}^{-2}$ , forward slope from Schegelsky - Ryskin fit [5], input  $\sigma_{tot}$  from PDG (2005)[3] (dashed curve), and input  $\sigma_{tot}$  from PDG (2013)[4] (solid curve), show good agreement with experimental values from Amos et al [46] and Abe et al [47] for  $|t| < 0.3\text{GeV}^2$ .

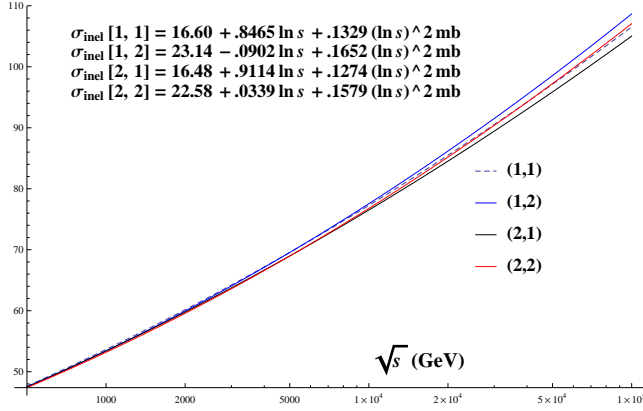


FIG. 5: Plots of  $pp$  inelastic cross sections  $\sigma_{inel}(q, M)$  computed from the model with  $q = 1$  and  $q = 2$  signifying inputs of  $\sigma_{total}(PDG - 2005)$  [3] and  $\sigma_{total}(PDG - 2013)$ [4] respectively and  $M = 1$  and  $M = 2$  signifying inputs of Okorokov [6] and Schegelsky - Ryskin [5] slopes respectively. Input Pomeron parameters are  $b_P = 3.8\text{GeV}^{-2}$ ,  $\alpha' = 0.07\text{GeV}^{-2}$ . Three parameter fits to these inelastic cross sections are also shown.

$B(2, s)$  by Schegelsky-Ryskin [5],

$$\begin{aligned} B(1, s) &= 8.81 + 0.396\ln s + 0.013(\ln s)^2 \text{ GeV}^{-2}, \\ B(2, s) &= 11.03 + 0.0286(\ln s)^2 \text{ GeV}^{-2}, \end{aligned} \quad (20)$$

where  $\sqrt{s}$  is in  $\text{GeV}$  units. For  $pp, \bar{p}p$  total cross sections I use the PDG fits of (2005) and (2013),

$$\begin{aligned} \sigma_{tot}^{(2005)}(s) &= 35.63 + 0.308\left(\ln\left(\frac{s}{28.94}\right)\right)^2 \text{ mb} \\ \sigma_{tot}^{(2013)}(s) &= 33.73 + 0.2838\left(\ln\left(\frac{s}{15.618}\right)\right)^2 \text{ mb}. \end{aligned} \quad (21)$$

**Elastic and inelastic cross sections.** The integrals over impact parameter needed to calculate  $\sigma_{el}$  can be

M=	2	2	2	2	2	2
$\sqrt{s}$ (GeV)	546	1800	7000	8000	13000	14000
$\sigma_{tot}$ (mb) PDG2013	61.303	76.2666	97.2354	99.5232	108.183	109.551
$D^2$ ( $\text{GeV}^{-2}$ )	37.4589	38.795	40.3161	40.4657	41.0094	41.0924
$B$ ( $\text{GeV}^{-2}$ )	15.5743	17.4574	19.9975	20.2701	21.2954	21.4566
$C$	0.368032	0.355357	0.341949	0.340686	0.336168	0.335489
$E$	0.0967198	0.144442	0.199302	0.2046	0.223619	0.226485
$R^2$ ( $\text{GeV}^{-2}$ )	174.777	180.545	195.35	197.148	204.121	205.243
$\sigma_{inel}/\sigma_{tot}$	0.784689	0.767591	0.747523	0.745582	0.738615	0.737567
$16\pi\sigma_{el}B/\sigma_{tot}^2$	1.07068	1.04127	1.01634	1.01425	1.0071	1.00607
$\rho$	0.143356	0.143121	0.137163	0.136402	0.133487	0.133025
$\sigma_{inel}$ (mb)	48.1038	58.5415	72.6858	74.2027	79.9053	80.8015

TABLE I: Detailed results at 546 GeV, 1.8 TeV, 7 TeV, 8 TeV, 13 TeV and 14 TeV from the model using inputs  $b_P = 3.8$ ,  $\alpha' = 0.07\text{GeV}^{-2}$ , PDG 2013 values of  $\sigma_{tot}(pp)$  [4], and Schegelsky-Ryskin extrapolations ( $M = 2$ , i.e.  $B = B(2, s)$ ) [5] for forward slopes. The output parameters  $C$  and  $E$  show explicitly that inelastic unitarity is obeyed. The output values of  $R^2$  show a slowly expanding size of the proton with increasing energy. The output results for  $\sigma_{inel}/\sigma_{tot}$ ,  $16\pi\sigma_{el}B/\sigma_{tot}^2$ , and  $\rho = \text{Re}F(s, t=0)/\text{Im}F(s, t=0)$ , which would be 1/2, 1 and 0 respectively in the black disk limit, give quantitative measures for deviations from that limit. The output  $\rho$  agrees with available experiments [49][50]. The output values of  $\sigma_{inel}$  agree within errors with Totem results [7][8] [9][10] and Atlas results [12][13][14][15] for  $pp$  scattering at 7 TeV and 8 TeV, and with the results of [47] for  $\bar{p}p$  scattering at 546 GeV and 1800 GeV. Model predictions at higher energies can be tested in future experiments.

M=	2	2	2	2	2	2
$\sqrt{s}$ (GeV)	546	1800	7000	8000	13000	14000
$\sigma_{tot}$ (mb) PDG2005	61.9255	77.2584	98.983	101.364	110.393	111.822
$D^2$ ( $\text{GeV}^{-2}$ )	37.4589	38.795	40.3161	40.4657	41.0094	41.0924
$B$ ( $\text{GeV}^{-2}$ )	15.5743	17.4574	19.9975	20.2701	21.2954	21.4566
$C$	0.388763	0.375374	0.361211	0.359876	0.355105	0.354387
$E$	0.0895596	0.138997	0.196895	0.20253	0.222814	0.225877
$R^2$ ( $\text{GeV}^{-2}$ )	180.005	183.611	197.264	198.984	205.713	206.802
$\sigma_{inel}/\sigma_{tot}$	0.779607	0.762221	0.741121	0.739053	0.731598	0.730472
$16\pi\sigma_{el}B/\sigma_{tot}^2$	1.08493	1.05165	1.02371	1.02138	1.01343	1.01228
$\rho$	0.144376	0.145604	0.1402	0.139456	0.136561	0.136098
$\sigma_{inel}$ (mb)	48.2776	58.888	73.3584	74.9136	80.7634	81.6831

TABLE II: Same as Table (I), but for input  $\sigma_{tot}(PDG - 2005)$ . Comparison shows that the predicted inelastic cross section at 7 TeV (8 TeV) increases by about 0.7 mb, when the input  $\sigma_{tot}$  increases by 1.8 mb (1.9 mb).

done exactly. We obtain,

$$\begin{aligned} \sigma_{el}(s) &= (\pi/2)C^2(s)D^2(s)(2 + (\beta'(s))^2) \\ &+ 4\pi R^2(s)E^2(s)(3 + 2\epsilon(s))/15 \\ &+ 2\pi R^2(s)C(s)E(s)\delta^{-3}(s) \left[ \exp(-2\delta(s)) \right. \\ &\times (-1 + 2\beta'(s)\sqrt{\epsilon(s)}(2\delta^2(s) + 3\delta(s) + 2)) + \\ &\left. (2\beta'(s)\sqrt{\epsilon(s)}(\delta(s) - 2) + 2\delta^2(s) - 2\delta(s) + 1) \right], \\ \delta(s) &\equiv R^2(s)/D^2(s), \quad \beta'(s) \equiv 4\pi\alpha'/D^2(s). \end{aligned} \quad (22)$$

**Predictions of the model versus experimental data for  $pp$  and  $\bar{p}p$  scattering.**

**Differential cross sections.** Remarkably, a single pair of values of the Pomeron parameters  $b_P, \alpha'$ ,

$$b_P = 3.8\text{GeV}^{-2}, \alpha' = 0.07\text{GeV}^{-2}. \quad (23)$$

gives very good agreement of model predictions in the entire range  $|t| < 0.3\text{GeV}^2$  with the experimental Totem

[7][8][9][10] and Atlas [12][13][14][15]  $pp$  differential cross sections at  $7TeV$  and  $8TeV$ , experimental  $\bar{p}p$  differential cross sections at  $546GeV$  from UA4 collaborations, D. Bernard et al [44] and M. Bozzo et al [45], and at  $1800GeV$  from Amos et al [46] and Abe et al [47]. (See also the compilation in [48]). This agreement is independent of the choice between PDG(2005) and PDG(2013) total cross sections, and the choice between slopes  $B(1, s)$  and  $B(2, s)$ . We exhibit this in Figs.(1, 2, 3, 4) for forward slope choice  $B = B(2, s)$  [5] and the two choices of total cross sections PDG (2005)[3] (dashed curve), and PDG (2013)[4] (solid curve). (Differential cross sections for  $(-t) > 0.3GeV^2$  are not used in determination of Pomeron parameters  $b_P, \alpha'$  as they make negligible contributions to  $\sigma_{el}$  in this energy range; e.g. in this model, about  $0.2mb$  at  $7TeV$  and  $8TeV$ .)

For the choice  $B = B(2, s)$  [5] and PDG (2013)[4] total cross sections, we give below three parameter fits to predicted differential cross sections in this range of  $t$  at c.m. energies upto  $14TeV$ ,

$$\begin{aligned} & \ln((d\sigma/dt)/(d\sigma/dt)_{t=0}) \\ &= 19.5t - 11.9t^2 + 43.5(-t)^3, 7TeV \\ &= 19.7t - 13.2t^2 + 47.3(-t)^3, 8TeV \\ &= 20.5t - 19.2t^2 + 64.2(-t)^3, 13TeV \\ &= 20.6t - 20.3t^2 + 67.2(-t)^3, 14TeV \end{aligned} \quad (24)$$

for ready comparisons with existing and future data.

**Inelastic cross sections.** Fig.(5) depicts the predicted inelastic cross sections up to  $100TeV$  and their asymptotic fits. Tables (I) and (II) give model parameters and detailed predictions from  $546GeV$  to  $14TeV$ , with input total cross sections  $PDG2013$  and  $PDG2005$  respectively. The predicted  $\rho = ReF(s, t)/ImF(s, t)|_{t=0}$  and the predicted inelastic cross sections (e.g. for input total cross section  $PDG2013$ ,  $\rho = 0.136$ ,  $\sigma_{inel} = 74.2mb$ , at  $8TeV$ ) are very close to available experimental values [49][50],[7][8] [9][10][12][13][14][15]. The predicted inelastic cross sections are fairly robust, changing by less than  $0.5mb$  in the range ( $7TeV, 14TeV$ ) when the slope parameter is changed from  $B(1, s)$  to  $B(2, s)$  and by less than  $1mb$  when the input  $\sigma_{tot}$  is changed from PDG (2005) to PDG (2013). Model results give  $\partial\sigma_{inel}/\partial B \sim 1.07mb GeV^2$ ,  $\partial\sigma_{inel}/\partial\sigma_{tot} \sim 0.46$ , and using input errors of PDG2013 fits, and  $\delta B \sim 0.3GeV^{-2}$  upto  $100TeV$  [5], I have the error estimate  $\delta\sigma_{inel} \sim .47 + .0021(\ln(s/15.618))^2 mb$ .

In the c.m. energy range from  $0.5TeV$  to  $100TeV$ , the model parameters are very well approximated by the following fits.

$$\begin{aligned} & Input \sigma_{tot}^{(2005)}(s) : \\ & M = 1 : E(s) = 0.987849 - 20.3797/x + 113.797/x^2 \\ & M = 1 : R^2(s) = 241.078 - 9.20435x + 0.375387x^2 \\ & M = 2 : E(s) = 0.861023 - 16.7296/x + 88.3041/x^2 \\ & M = 2 : R^2(s) = 245.408 - 11.3716x + 0.487702x^2 \end{aligned} \quad (25)$$

$$Input \sigma_{tot}^{(2013)}(s) :$$

$$\begin{aligned} & M = 1 : E(s) = 0.936736 - 18.91/x + 104.505/x^2 \\ & M = 1 : R^2(s) = 214.735 - 6.85598x + 0.320973x^2 \\ & M = 2 : E(s) = 0.812299 - 15.3352/x + 79.6064/x^2 \\ & M = 2 : R^2(s) = 220.921 - 9.20272x + 0.437436x^2 \end{aligned}$$

where,  $x \equiv \ln s$ .

Remarkably, fits for input  $\sigma_{tot}^{(2005)}(s)$  show that the choice  $M = 1$  gives  $E(s)$  which is barely below the unitarity limit for  $s \rightarrow \infty$ . The inelastic cross section fits in Figure 5 yield ,

$$\begin{aligned} & Input \sigma_{tot}^{(2013)}(s) : \\ & M = 1 : \frac{\sigma_{inel}}{\sigma_{tot}} \rightarrow 0.449; M = 2 : \frac{\sigma_{inel}}{\sigma_{tot}} \rightarrow 0.556 \\ & Input \sigma_{tot}^{(2005)}(s) : \\ & M = 1 : \frac{\sigma_{inel}}{\sigma_{tot}} \rightarrow 0.431; M = 2 : \frac{\sigma_{inel}}{\sigma_{tot}} \rightarrow 0.536 \end{aligned} \quad (27)$$

These results are close to the black disk value of  $1/2$  favoured by BH [39][40]. Recent detailed analysis of high energy data [51] concluded that, although consistent with experimental data, the black disk does not represent an unique solution.

**Phenomenological lowest t-channel singularity.** If continued to complex  $t$ ,  $|F(s, t)|$  given by this model is bounded by  $Const.s^2$  for  $s \rightarrow \infty$  and

$$|t| < t_1 = \min[(1/\alpha'), \lim_{s \rightarrow \infty} (\ln s/R(s))^2]. \quad (28)$$

Jin and Martin [52] proved that for  $|t| < t_0$ , where  $t_0$  is the lowest  $t$ -channel singularity, twice subtracted dispersion relations in  $s$  hold. Hence  $t_1$  may be thought of as a phenomenological lowest  $t$ -channel singularity. Using the formulae for  $R^2(s)$  given above,

$$\begin{aligned} & Input \sigma_{tot}^{(2013)}(s) : \\ & M = 1 : \sqrt{t_1} = 1.765 GeV; M = 2 : \sqrt{t_1} = 1.512 GeV; \\ & Input \sigma_{tot}^{(2005)}(s) : \\ & M = 1 : \sqrt{t_1} = 1.632 GeV; M = 2 : \sqrt{t_1} = 1.432 GeV. \end{aligned}$$

Our  $\sqrt{t_1} \sim 1.4 - 1.8GeV$  is reminiscent of , but different from the glue-ball mass of BH [39][40]. Given the instability of analytic continuations, its main function is to suggest that the usual Lukaszuk-Martin bound [20] is quantitatively poor as it assumes lack of  $t$ -channel singularities only upto  $4m_\pi^2$  which is much smaller than  $t_1$ .

**Conclusion.** I presented an analytic formula for the high energy elastic amplitude  $F(s, t) = F^{(1)}(s, t) + F^{(2)}(s, t)$  given by Eqns. (7,18) for  $\sqrt{s} > 100GeV$ , exhibiting Froissart bound saturation, AKM scaling [1][2], inelastic unitarity, predicting differential cross sections for  $(-t) < 0.3GeV^2$  and total inelastic cross sections, at  $546GeV$ ,  $1800GeV$ ,  $7TeV$  and  $8TeV$  in agreement with experimental results, as well as the real parts and inelastic cross sections upto  $100TeV$ . An 'effective'  $t$ -channel

singularity at  $\sqrt{t} \sim 1.4 - 1.8 \text{ GeV}$  is suggested by analytic continuation to positive  $t$ . Detailed tables and graphs of model parameters, real parts and cross sections upto  $100 \text{ TeV}$  will be published separately. The 'grey disk' component could be generalized using a smoother impact parameter cut-off, i.e.  $n > 1$  in Eqn. (5).

**Acknowledgements.** I presented an earlier version with a black disk second component in 2015 to André Martin and T.T. Wu at CERN; their insistence that a sharp impact parameter cut-off is too 'brutal' led to the black disk being replaced by the grey disk. I thank G.

Auberson for remarks concerning instability of analytic continuation, D. Atkinson, G. Mahoux and V. Singh for helpful comments on the manuscript; I also thank Gilberto Colangelo and Heiri Leutwyler for very helpful discussions, and a seminar invitation at Univ. of Bern, and Irinel Caprini and Juerg Gasser for discussions on a very stimulating ansatz for high energy pion-pion scattering [53]. I thank the referees for the crucial suggestion of comparison with the latest differential cross section data and the Indian National Science Academy for an INSA senior scientist grant.

- 
- [1] G. Auberson, T. Kinoshita and A. Martin, Phys. Rev. D **3**, 3185 (1971).
  - [2] G. Auberson and S. M. Roy, Nucl. Phys. **B117**, 322 (1976).
  - [3] S. Eidelman et al (Particle data Group) Phys. Lett. **B592**, 1 (2004) and 2005 partial update, [http://pdg.lbl.gov/2005, Table 40.2](http://pdg.lbl.gov/2005/Table 40.2).
  - [4] J. Beringer et al (Particle data Group) Phys. Rev. **D86**, 010001 (2012) and 2013 partial update, <http://pdg.lbl.gov/2013, Table 50>.
  - [5] V. A. Schegelsky and M. G. Ryskin, Phys. Rev. **D85**, 094024 (2012).
  - [6] V. A. Okorokov, arXiv:1501.01142 v2[hep-ph] 23 May, 2015.
  - [7] Totem collaboration, G. Antchev et al, Europhys. Lett. **96**, 21002 (2011).
  - [8] Totem collaboration, G. Antchev et al, Europhys. Lett. **101**, 21004 (2013); CERN-PH-EP-2012-239.
  - [9] Totem collaboration, G. Antchev et al, Phys. Rev. Lett. **111**, 012001 (2013).
  - [10] Totem collaboration, G. Antchev et al, Nucl. Phys. B **899**, 527 (2015); arXiv:1503.08111 [hep-ex].
  - [11] CMS collaboration, Phys. Lett. **B722**, 5 (2013); presentation at EPS-HEP conference, Vienna, 22-29 July (2015).
  - [12] Atlas collaboration, Nature Comm. **2**, 463 (2011).
  - [13] Atlas collaboration, Nucl. Phys. B **889**, 486 (2014); arXiv:1408.5778v2 [hep-ex].
  - [14] Atlas collaboration, ATLAS-CONF-2015-038.
  - [15] Atlas collaboration, CERN-EP-2016-158 (25 July 2016); arXiv:1607.06605v1 [hep-ex] (submitted to Phys. Lett. B).
  - [16] Alice collaboration, ArXiv:1208.4968 (2012).
  - [17] Pierre Auger collaboration, Phys. Rev. Lett. **109**, 062002 (2012).
  - [18] M. Froissart, Phys. Rev. **123**, 1053 (1961).
  - [19] A. Martin, Nuov. Cimen. **42**, 930 (1966).
  - [20] L. Lukaszuk and A. Martin, Nuov. Cimen. **52A**, 122 (1967).
  - [21] S. M. Roy, Phys. Reports, **5C**, 125 (1972).
  - [22] J. Kupsch, Nuovo Cim. **71A**, 85 (1982).
  - [23] H. Cheng and T. T. Wu, Phys. Rev. Letters **24**, 1456 (1970).
  - [24] C. Bourrely, J. Soffer, and T. T. Wu, Phys. Rev. **D19**, 3249 (1979).
  - [25] C. Bourrely, J. Soffer, and T. T. Wu, Nucl. Phys. **B247**, 15 (1984).
  - [26] C. Bourrely, J. Soffer, and T. T. Wu, Z. Phys. C **37**, 369 (1988).
  - [27] C. Bourrely, J. Soffer, and T. T. Wu, Eur. Phys. J. **C28**, 97 (2003).
  - [28] C. Bourrely, J. Soffer, and T. T. Wu, Eur. Phys. J. **C71**, 1061 (2011).
  - [29] M. M. Block et al, Phys. Rev. **D60**, 054024 (1999).
  - [30] M. M. Block, Phys. Reports, **436**, 71 (2006).
  - [31] M. M. Block and F. Halzen, Phys. Rev. D **83**, 077901 (2011).
  - [32] M. M. Islam et al, Int. J. Mod. Phys. A **21**, 1 (2006).
  - [33] A. Martin, Phys. Rev. **D80**, 065013 (2009).
  - [34] T. T. Wu, A. Martin, S. M. Roy and V. Singh, Phys. Rev. **D84**, 025012 (2011).
  - [35] A. Martin and S. M. Roy, Phys. Rev. D **89**, 045015 (2014).
  - [36] A. Martin and S. M. Roy, Phys. Rev. **D91**, 076006 (2015).
  - [37] R. F. Avila, P. Gauron and B. Nicolescu, Eur. Phys. J. **C49**, 581 (2007).
  - [38] E. Martynov and B. Nicolescu, Eur. Phys. J. **C56**, 57 (2008).
  - [39] M. M. Block and F. Halzen, Phys. Rev. Lett. **107**, 212002 (2011).
  - [40] Phys. Rev. D **86**, 051504(R) (2012).
  - [41] N. N. Khuri and T. Kinoshita, Phys. Rev. **137**, B720 (1965).
  - [42] A. Martin, Lett. Nuovo Cimento **7**, 811 (1973).
  - [43] A. Martin, CERN-TH/97-23 (1997).
  - [44] D. Bernard et al, UA4 collaboration, Phys. Lett. **B198**, 583 (1987).
  - [45] M. Bozzo et al, UA4 collaboration, Phys. Lett. **B147**, 385 (1984).
  - [46] N. A. Amos et al, Phys. Lett. **B247**, 127 (1990).
  - [47] F. Abe et al, Phys. Rev. D **50**, 5518 (1994) and Phys. Rev. D **50**, 5550 (1994).
  - [48] J. R. Cudell, A. Lengyel, E. Martynov, Phys. Rev. D **73**, 034008 (2006) and arXiv: hep-ph/0511073.
  - [49] COMPETE Collaboration, J. R. Cudell et al, Phys. Rev. Lett. **89**, 201801 (2002).
  - [50] COMPETE Collaboration, J. R. Cudell et al, Phys. Rev. D **65**, 074024 (2002).
  - [51] D. A. Fagundes, M. J. Menon and P. V. R. G. Silva, Nucl. Phys. **A946**, 194 (2016).
  - [52] Y. S. Jin and A. Martin, Phys. Rev. **135B**, 1375 (1964).
  - [53] I. Caprini, G. Colangelo, and H. Leutwyler, Eur. Phys. J. **C72**, 1860, (2012).